ASSESSMENT OF A CFD MODEL FOR THE SIMULATION OF FAST FILLING OF HYDROGEN TANKS WITH PRE-COOLING

Melideo D. [1], Baraldi D. [1], Galassi M.C. [1], Ortiz Cebolla R. [1], Acosta Iborra B. [1], Moretto P. [1]
[1] European Commission Joint Research Centre, Institute for Energy and Transport, Westerduingweg 3, P.Box 2, Petten, 1755 ZG, Petten, Netherlands.
daniele.melideo@ec.europa.eu, daniele.baraldi@jrc.nl

ABSTRACT

High gas temperatures can be reached inside a hydrogen tank during the filling process because of the large pressure increase (up to 70-80 MPa) and because of the short time (~3 minutes) of the process. High temperatures can potentially jeopardize the structural integrity of the storage system and one of the strategies to reduce the temperature increase is to pre-cool the hydrogen before injecting it into the tank. Computational Fluid Dynamics (CFD) tools have the capabilities of capturing the flow field and the temperature rise in the tank. The results of CFD simulations of fast filling with pre-cooling are shown and compared with experimental data to assess the accuracy of the CFD model.

1.0 INTRODUCTION

Nowadays drivers are used to re-fill the vehicle tank in few minutes with conventional fuel like gasoline and diesel. They have similar expectations towards a new technology like hydrogen powered vehicles. The requirement of a reasonable short filling time introduces a new challenge since the increase of temperature due to the quick compression inside the tank e.g. from low pressure up to 700 bars could be harmful for the mechanical properties of the tank material. Because of this reason, the maximum allowed temperature inside tanks is set to 85 C - 358 K by the majority of the international standards and regulations (e.g. the European regulation [1], the SAE [2] and the international standard ISO 15869 [3]). Moreover the higher is the temperature, the smaller is the gas density and the smaller is the amount of gas that can be filled inside the tank. One of the technological solutions that were envisaged to tackle the issue of high temperature is to decrease the temperature of the gas going inside the tank by means of a heat exchanger. The process is called pre-cooling and in this work the pre-cooling is investigated both from the experimental and numerical point of view.

Given the importance of the re-fuelling issue for the deployment of hydrogen technology in the automotive sector, the number of papers with investigation on the fast filling process that have been published in the last decade has increased constantly [4-13].

The results that are presented hereafter are part of a validation programme of CFD modeling strategy that has been going on since 2011 [10-13]. The novelty in this specific investigation is that for the first time an experiment with pre-cooling has been reproduced by the same CFD modeling strategy that was previously applied to capture other experiments without pre-cooling [10-13]. A CFD model must be capable of reproducing experiments within a wide range of conditions for the specific application before it can be used for numerical analyses of the phenomena with a certain level of confidence in the accuracy of the model. In this context, the aim of the study is an extension of the model performance evaluation to include pre-cooling conditions in the validation programme. The difference in the results between a real gas equation and the ideal gas equation, and the effect of different inlet temperatures were also investigated numerically.

2.0 EXPERIMENT

The selected experiment was carried out at JRC Institute for Energy (IE) in the compressed hydrogen Gas Tanks Testing Facility (GasTeF), which represents an EU reference laboratory on safety and

performance assessment of high-pressure hydrogen storage tanks [14]. The facility is sited in a half-buried strongly reinforced concrete bunker with annexed gas storage area. In the test room, a pressure vessel contains the component to be tested; the fuel tank is placed into a sleeve which, can be filled with inert gas, becoming a safety chamber where no oxidizer is present in the case of a leak of hydrogen from the tank. Moreover the sleeve allows for permeation measurements as it works as a containment where the hydrogen that escapes from the tank by permeation can be collected and measured. The sleeve temperature can be varied from ambient to100°C, while the pressure in the tank can be increased up to ca. 85 MPa. Cycling tests aim at providing information on long-term mechanical and thermal behavior of high-pressure tanks and their safety performance. The tests consist of a fast filling (few minutes), simulating the refueling at the service station, followed by a slow emptying phase, representing the gas consumption. This transients' combination can be repeated up to 1000 times to simulate the typical life of tanks. During the tests, several parameters are monitored in order to evaluate tank performance: external temperature, temperature and deformation of the tank walls as well as the possible leakage or permeation of hydrogen and internal gas temperature at different positions. More details on available data can be found in [15].

In Figure 1, the geometry of the tank is shown with the positions of the thermocouples. Tanks for automotive applications are composed of a carbon fiber composite wrapping and a liner that can be made of metal (type 3 tank) or polymers (type 4 tank). In the selected test the fast filling process of a type IV tank up to 72MPa is considered. Measured temperatures at specific points in the tank are compared with predicted values during the filling transient, in order to validate the CFD modeling strategy. Working conditions of selected tests are summarized in Table 1; the corresponding transient pressure and temperature history measured at the tank inlet are shown in Figure 2. The initial drop and the final increase in the temperature profile are due to the switch on and the switch off of the heat exchanger during the experiment respectively. The experimental pressure and temperature history was considered as boundary condition in the inlet in the simulation.

In Figure 3, the temperature history of 6 sensors in the tank is illustrated. Temperature differences in the gas in different position are negligible during the filling transient and the temperature distribution inside the tank can be considered as uniform in that stage. The hydrogen jet creates strong recirculation inside the tank which generates a homogenous temperature field. Therefore only one thermocouple position can be taken into account for the comparison between experimental data and simulation results as being representative of the gas temperature history in the tank. The selected thermocouple TC3 is placed in the upper region of the tank as shown in Figure 1. After the end of the filling, the convective field generated by the jet disappears from the domain and thermal stratification takes place.

Table 1: Initial conditions

	H_2 P_{in} [MPa]	H_2 P_{fin} [MPa]	$t_{filling}$ [s]	T_{sleeve} [°C]	H_2 T_{ini} [°C]
Test H2 10122010	2.2	71.7	200	15	21

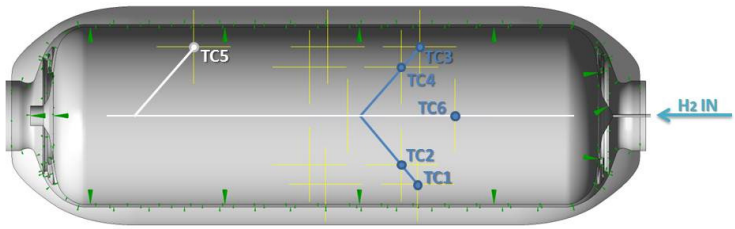

Figure 1: Tank geometry and thermocouples position.

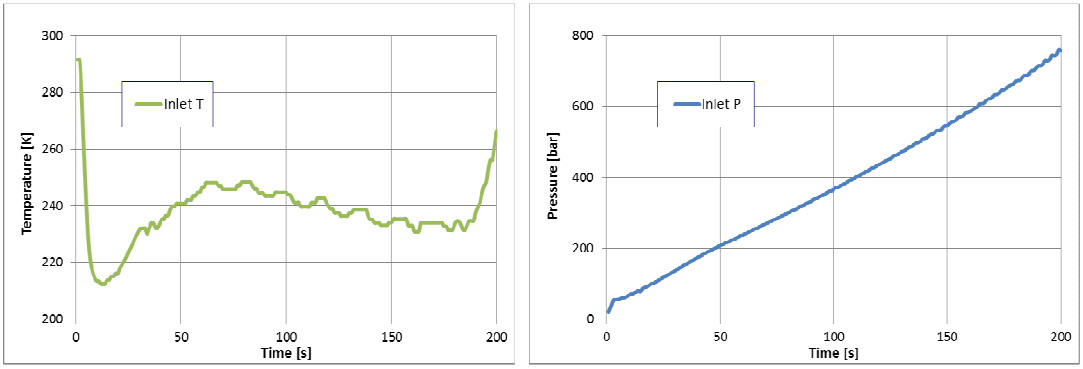

Figure 2: Pressure and temperature history at tank inlet.

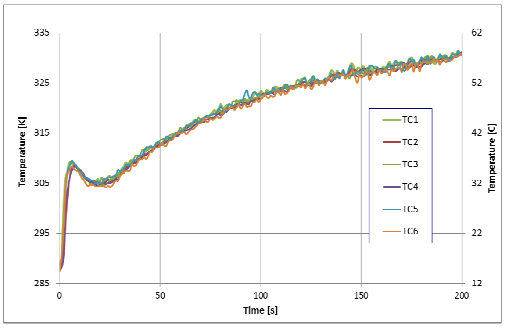

Figure 3: Temperature history in the experiment.

3.0 SIMULATION RESULTS

The computational meshes were generated with the Pointwise V17.0 software [16]. The numerical simulations were performed with the commercial CFD software ANSYS CFX V14.0 [17]. CFX includes also a conjugate heat transfer (CHT) capability which was applied in the present study, allowing calculation of pure thermal conduction through solid materials coupled with the changing temperature in the fluid. The numerical time scheme is based on a Second Order Backward Euler scheme. The high resolution scheme of CFX was selected for the advection terms. Further details on the numerical scheme can be found in ANSYS CFX manual [17]. A residual convergence criterion for RMS (root mean square) mass-momentum equations of 10^{-4} was used to ensure the attainment of negligible iteration errors.

3.1 Computational model

The computational model is composed of 4 sub-domains: a fluid domain representing the tank interior filled by the hydrogen, a solid domain representing the internal plastic liner, a solid domain representing the external composite carbon fiber wrap, and a solid domain representing the two stainless steel bosses at the tank ends. The computational grids were generated as a hybrid mesh: the inlet pipe and solid domains were composed of hexahedral cells, while the remaining fluid domain was generated with tetrahedral elements.

A real gas equation of state for the evaluation of hydrogen properties (Aungier Redlich-Kwong [18]) was selected to take into account compressibility effects at high pressures. The turbulence closure is achieved with a modified k- ε model [19] in order to reduce the jets spreading rate over-prediction of the standard model [19-21]. In the modified model, the value of the constant coefficient, $C_{\varepsilon 1}$ of the production term in the dissipation equation was changed from 1.44 to 1.52 [19]. A non-slip boundary condition (v=0 m/s) was applied at all walls. The experimental pressure and temperature profiles were imposed as boundary condition at the tank inlet where a pressure boundary condition was selected. A constant heat transfer coefficient (6 W/m^2K [22]) was imposed at the outer tank and bosses walls, to evaluate the heat transfer to the environment. Initial conditions were defined by the initial experimental temperature and pressure within the tank, which were assumed to be uniform (p= 2.2 MPa, T= 21° C). Tank walls were considered to be initially at the same temperature as the gas; the ambient temperature (T = 15 ° C) was assumed to be constant.

3.2 2D-3D simulations

In previous fast filling studies from the same group of authors [10-13], a 3D computational mesh was generated. Although the 3D computational model represents accurately the geometry and although it was shown to be capable of reproducing with good agreement the experimental data, from the point of view of the computational resources it has almost prohibitively cost, requiring up to several weeks for a complete run. In view of that drawback, the possibility to use 2D computational meshes was successfully investigated for the first time for this CFD model. It must be emphasized that the 3D mesh and the 2D mesh were built starting from the same plane surface mesh in order to reduce any possible difference in the mesh resolution and in the cell density distribution in the two computational grids. The 2-D mesh is axi-symmetric mesh. As illustrated in Figure 4, the temperature histories for the 3D and 2D meshes are almost completely overlapping. It must be emphasized that the 2D axi-symmetric approach can be used during the filling stage but it is not appropriate in the following stages since the process can not be considered as axi-symmetric when stratification occurs inside the tank after the end of the filling.

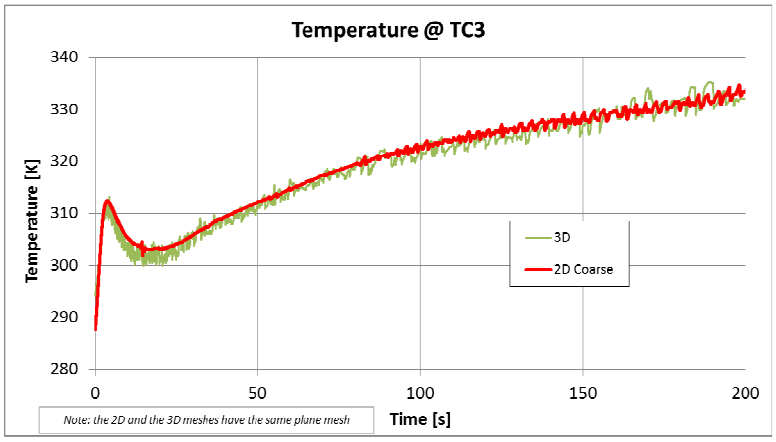

Figure 4: Comparison of simulation results with 3D and 2D computational grids. Temperature versus time in position TC3.

3.3 Grid sensitivity analysis

Due to the extremely long computer run-time for the 3D mesh, the grid sensitivity analysis was performed only on the 2D mesh. Three different meshes were generated. In Table 2, details about the grids can be found. An initial relatively coarse mesh was built with a total of 23668 nodes. The second mesh was built adding to the first mesh a thin layer of hexahedral cells on the fluid domain that is in contact with the interior walls of the tank to increase the mesh resolution in a crucial region for the heat transfer between the fluid and the solid. The total number of nodes for the second mesh is 27548. Finally a third mesh with much finer resolution was generated with 94436 nodes. As shown in Figure 5, the differences in the results from the calculations with the 3 meshes are negligible, being a few degrees for the final maximum temperature.

Table 2: Number of nodes in computational grids.

	Number of Nodes				
2D MESHES	Tank	Flange	CF Composite	Liner	**TOT**
Fine	59090	8676	21126	5544	**94436**
Coarse	11904	3568	4788	3408	**23668**
B. Layer	15784	3568	4788	3408	**27548**
	Tank	Flange	CF Composite	Liner	**TOT**
3D MESH	98148	57000	79002	56232	**290382**

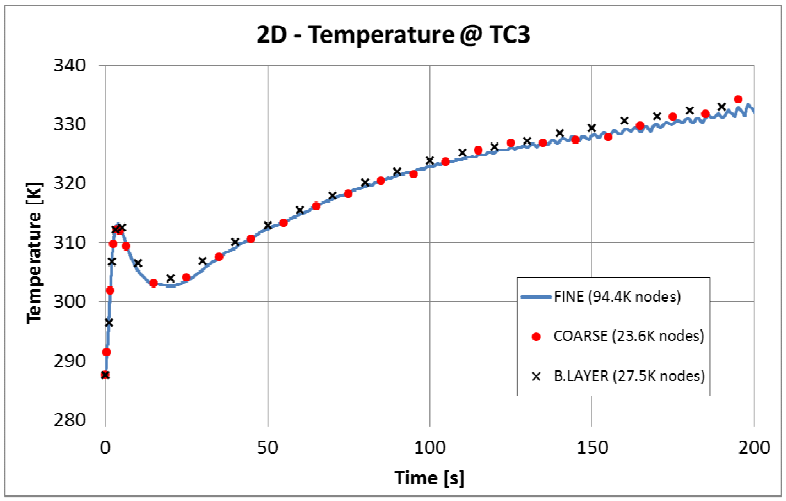

Figure 5 Comparison of simulation results with 3 different meshes. Temperature versus time in position TC3.

3.4 Simulation results

The good agreement between experimental data and simulation results is shown in Figure 6. Also in the simulation (like in the experiment) it was confirmed that the temperature field inside the tank during the filling can be considered as uniform. Therefore it is sufficient to show the comparison for only one sensor position.

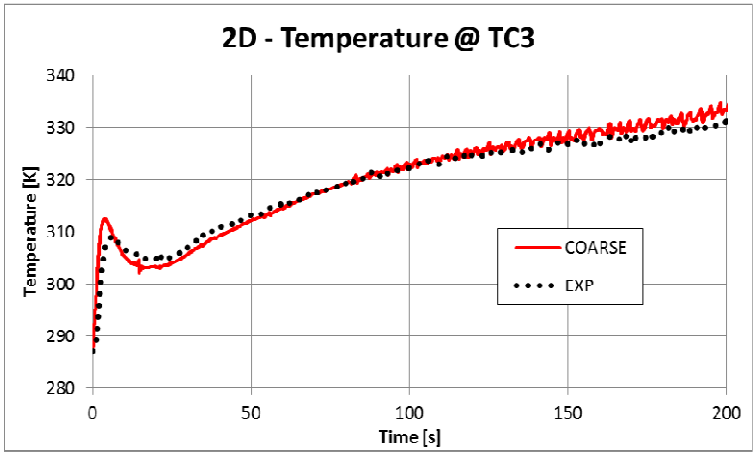

Figure 6: Comparison experimental data and simulation results for the temperature history.

The calculations were performed with the Aungier Redlich Kwong equation [18]. Other 3 real-gas equation of states were considered (standard Redlich Kwong [23] , Soave Redlich Kwong [24], and Peng-Robinson [25]) without generating any relevant difference in the temperature histories. Finally a calculation with the ideal gas equation of state was carried out and that produced significant difference in the results as shown in Figure 7. In the first few seconds of the simulations, the real gas and the ideal gas histories are almost overlapping, as it can be expected because the difference between the two equations of state is negligible at low pressure and it increases with increasing pressure as it is illustrated in the figure. At the end of the simulation, the maximum temperature difference between the two cases is found and it is about 13 K.

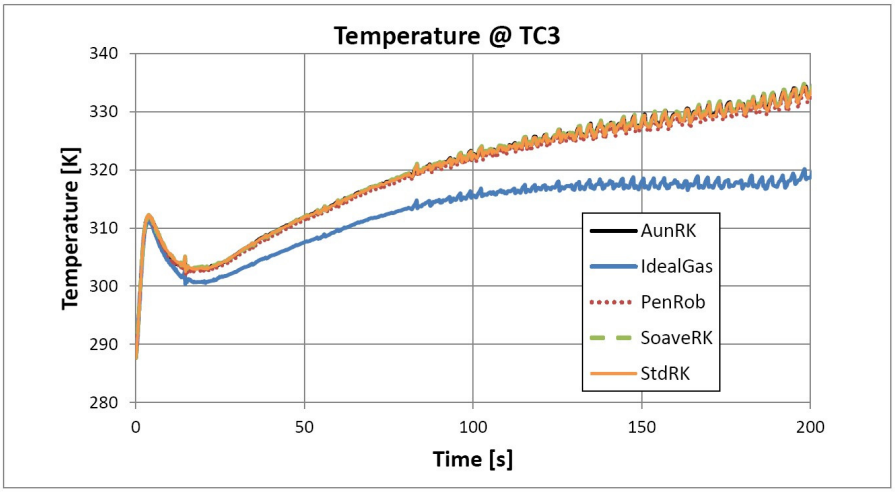

Figure 7: Temperature history with the real gas equation of state and with the ideal gas equation of state.

The heat exchanger was switched on at the beginning of the filling procedure and switched off towards the end during the experiment. That is clearly shown by the initial sharp drop and final rise of temperature in the inlet gas temperature history in Figure 8 (left-hand side). The temperature history between those two events is strongly affected by the efficiency of the heat exchanger. In order to investigate a filling procedure with an "ideal" heat exchanger that is capable to keep constant the required temperature along the whole process, four additional simulations were performed. The inlet gas temperature was changed to -40 ° C, -20 ° C, 0 ° C, and 15 ° C as described in Figure 8 (left-hand side). The effect of changing the inlet gas temperature is illustrated on the right hand side of the same figure and as it was expected higher hydrogen temperatures corresponds to a higher inlet temperature. With -40 ° C and -20 ° C inlet temperature, the maximum temperature at the end of the filling stage is below 85 ° C, while with 0 ° C that threshold is reached. With 15 ° C, the threshold is overcome by about 10 ° C. It can also be noted that with the changing inlet temperature in the experiments, the maximum final temperature is very close to the case with a constant – 40 ° C temperature.

The linear correlation between the inlet pre-cooling temperature and the maximum temperature at the end of the filling process is shown in Figure 9. This finding is consistent with the linear correlation that was highlighted for a type 3 cylinder between the averaged temperature rise and different ambient temperature [26]. The effect of the inlet gas temperature has an effect also on the averaged flow mass rate and on the total mass that is injected into the tank, as shown in Table 3. The higher the inlet temperature the lower is the gas density and the lower is the gas that can be contained in the tank at the same pressure. In this specific case, the difference can be as high as 7% with the reference case that

corresponds to the experiment. The total mass decreases almost linearly with increasing pre-cooling temperature as shown in Figure 10.

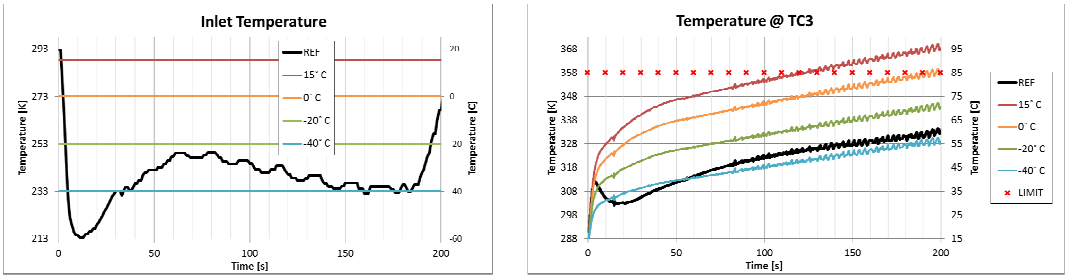

Figure 8: Inlet gas temperature versus time (left-hand side). Tank gas temperature history (right-hand side).

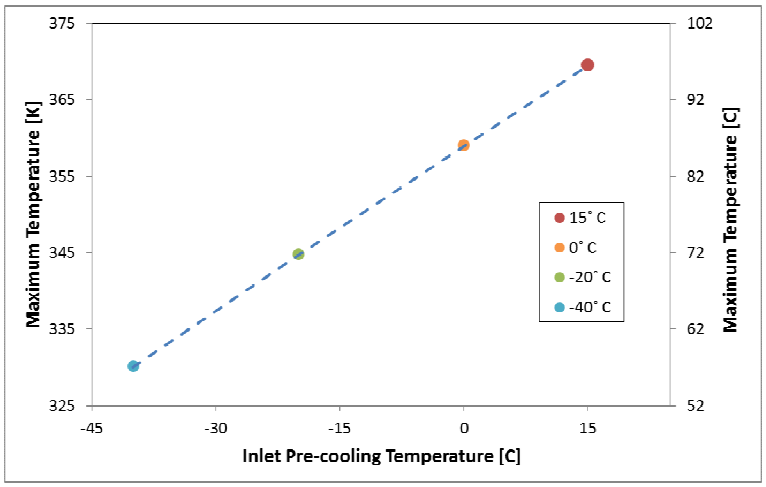

Figure 9: Maximum temperature in the tank versus maximum pre-cooling temperature.

Table 3: Averaged mass flow rate and total mass.

	REF	**-40° C**	**-20° C**	**0° C**	**15° C**
AVG Mass Flow [kg/s]	0.00522	0.00531	0.00516	0.00497	0.00485
Total Mass [kg]	1.045	1.062	1.031	0.994	0.971
Diff %	-	+1.63	-1.34	-4.88	-7.08

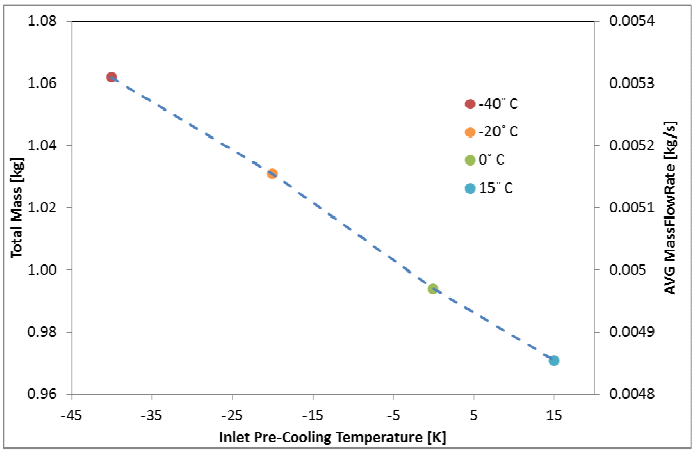

Figure 10: Total mass in the tank versus maximum pre-cooling temperature.

4.0 CONCLUSIONS

As part of a validation programme of a CFD modeling strategy for fast filling of hydrogen tanks, a new model assessment exercise was performed by comparison of experimental data and simulation results for a case with pre-cooling of the gas for a type 4 70 MPa tank. The main conclusions were:

- the CFD results from a 2D axi-symmetric mesh are as accurate as those in a 3D mesh during the filling process.
- grid independency of the CFD results was achieved
- the agreement between experimental date and simulation results is satisfactory for the gas temperature inside the tank. The difference between the simulation and the experiment is in the order of 2-3 degrees
- it is necessary to consider a real gas equation of state instead of the ideal gas equation in order not to significantly underestimate the maximum temperature inside the tank
- a linear correlation exists between the pre-cooling temperature and the maximum gas temperature at the end of the filling
- the effect of different pre-cooling temperature on the averaged mass flow rate and total mass of gas that is injected inside the tank were quantified.

ACKNOWLEDGEMENT

The authors would like to acknowledge and thank all colleagues working on GasTeF facility, Harskamp Frederik, and Bonato Christian for the information on the experimental facility and for their support.

REFERENCES.

1. Commission Regulation (EU) No 406/2010 of 26 April 2010 implementing regulation (EC) No 79/2009 on type-approval of hydrogen-powered motor vehicles. Off J Eur Union 18.05.2010. L 122/1e107.
2. SAE J2579. Technical information report for fuel system in fuel cells and other hydrogen vehicles, revised; SAE International. January 2009.
3. International Standard Organization. Gaseous hydrogen and hydrogen blends e land vehicle fuel tanks. ISO/TS 15869; 2009.
4. Dicken, C.J.B., Merida, W., 2007. Modeling the transient temperature distribution within a hydrogen cylinder during refueling. Numerical Heat Transfer, Part A: Applications 53, 685–708.
5. Kim, S.C., Lee, S.H., Yoon, K.B., 2010. Thermal characteristics during hydrogen fueling process of type IV cylinder. International Journal of Hydrogen Energy 35, 6830–6835.
6. Suryan A., Kim H.D., Setoguchi T., 2012 Three dimensional numerical computations on the fast filling of a hydrogen tank under different conditions. International Journal of Hydrogen Energy 37,7600-7611.
7. Y. Takagi, N. Sugie, K. Takeda, Y. Okano, T. Eguchi, K. Hirota, Numerical investigation of the thermal behaviour in a hydrogen tank during fast filling process. Asme/Jsme 2011, Honolulu,Hawaii, USA.
8. Zhao, L., Liu, Y., Yang, J., Zhao, Y., Zheng, J., Bie, H., Liu, X., 2010. Numerical simulation of temperature rise within hydrogen vehicle cylinder during refueling. International Journal of Hydrogen Energy 35, 8092–8100.
9. Zhao, Y., Liu, G., Liu, Y., Zheng, J., Chen, Y., Zhao, L., Guo, J., He, Y., 2012. Numerical study on fast filling of 70 MPa type III cylinder for hydrogen vehicle. International Journal of Hydrogen Energy.
10. Heitsch M, Baraldi D, Moretto P. Numerical investigations on the fast filling of hydrogen tanks. Int J Hydrogen Energy **36**, 2011, pp 2606-2612.
11. Galassi MC, Baraldi D, Iborra BA, Moretto P. CFD analysis of fast filling scenarios for 70 MPa hydrogen type IV tanks. Int J Hydrogen Energy **37**, 2012, pp 6886-6892.
12. Galassi M. C., Acosta-Iborra B., Baraldi D., Bonato C., Harskamp F., Frischauf N., Moretto P., Onboard Compressed Hydrogen Storage: Fast Filling Experiments and Simulations. Energy Procedia **29,** 2012, pp 192 – 200.
13. Galassi M.C., Papanikolaou E., Heitsch M., Baraldi D., Acosta Iborra B., Moretto P., Validation of CFD models for hydrogen fast filling simulations. Int J Hydrogen Energy. In press.
14. Acosta, B., Moretto, P., Frischauf, N., Harskamp, F., GASTEF: The JRC-IE Compressed Hydrogen Gas Tanks Testing Facility, Proceedings of the Eighteenth World Hydrogen Energy Conference, 16-21 May 2010, Essen.
15. Acosta, B., Moretto, P., Frischauf, N., Harskamp, F., Bonato, C., Fast Filling and Permeation Experiments at the JRC-IE GasTeF Facility, Proceedings of the Forth International Conference on Hydrogen Safety, 12-14 September 2011, San Francisco.
16. Pointwise User Manual. Release 17.0. Pointwise Inc.; 2012.
17. ANSYS CFX User's Guide. Release 14.0. ANSYS Inc.; 2012.
18. Aungier R. H. A Fast, Accurate Real Gas Equation of State for Fluid Dynamic Analysis Applications. Journal of Fluids Engineering. 117. 277–281. 1995.
19. Ouellette P, Hill PG. Turbulent transient gas injections. J Fluids Eng **122**, 2000, pp743-753.
20. Pope SB. An explanation of the turbulent round-jet/plane-jet abnormality. AIAA J **16**, 1978, pp 279. Technical note.
21. Magi V, Iyer V, Abraham J. The k-e model and computed spreading in round and plane jets. Num Heat Transfer J **40**, 2001, pp 317-334.

22. Zhao L, Liu Y, Yang J, Zhao Y, Zheng J, Bie H, et al. Numerical simulation of temperature rise within hydrogen vehicle cylinder during refueling. Int J Hydrogen Energy **35**, 2010, 8092-9000.
23. Redlich O, Kwong JNS. On the thermodynamics of solutions: V. An equation of state: fugacity of gaseous solutions. Chem Rev **44,**1949, pp 233–244.
24. Soave G. "Equilibrium Constants from a modified Redlich-Kwong equation of State". Chemical Engineering Science. **27**, 1972, 1197.
25. Peng D.Y., Robinson D.B. A New Two-Constant Equation of State. Industrial and Engineering Chemistry: Fundamentals. **15,** 1976, 59–64.
26. Zheng JY, Liu XX, Xu P, Liu PF, Zhao YZ, Yang J. Development of high pressure gaseous hydrogen storage technologies. Int J Hydrogen Energy **37**, 2012, 1048-57.